Complexity Project: The Oslo Model

Georgios Hajivassiliou
CID: 01068099

14th February, 2019

Abstract: A computational implementation of the Oslo Model is run for systems of sizes $L = 4, 8, 16, 32, 64, 128,$ and 256 with the capability of measuring the height and slope at each site and recording avalanches and their sizes. The implementation was validated with a series of tests. This is followed by a series of measurements related to the height of the pile which demonstrates that, although the systems of different sizes follow similar dynamics, there are finite-scaling effect which are quantified in the end of the section. The next and last section consider avalanche-size probability. It is successfully demonstrated that the systems follow a power law and are hence scale-free in that respect.

Word count: 2467 words in report (excluding front page, figure captions, table captions, acknowledgement and bibliography).

1 Introduction

The Oslo Model (introduced in 1996 [1]) is one of the simplest models displaying self-organised criticality. This is an example of a system that displays behaviour much richer than the sum of its parts. Similar systems include, rainfall, earthquakes and the stock market. Hence, despite being governed by a very simple algorithm, the model displays rich non- trivial behaviour. Here, Oslo Model systems of various sizes are created and ran while different observables such as their height, average slope and avalanche size are measured in order to analyse their scaling properties within the concepts of self-organised criticality and finite-size scaling. A system of size L consists of L sites labeled by $i = 1, 2, ..., L$. At each site, the number of grains is the height h_i and its difference from the next site $(h_i - h_{i+1})$ is the slope z_i. Each site is assigned a random threshold slope ($z_i^{th} = 1$ or 2) and the system is driven by adding grains to site $i = 1$. When the slope $z_i > z_i^{th}$ then the site topples (relaxes), i.e. the grain is moved to the next site, and the threshold slope of this site is randomly assigned a new value. Time is measured as the amount of times the system has been driven. All of this is captured in the Oslo Model algorithm below [2]:

1. *Initialisation.* Prepare the system in the empty configuration with $z_i = 0$ for all i and chose random initial threshold slopes $z^t h_i \in 1, 2$ for all i.

2. *Drive.* Add a grain at the left-most site i = 1:

$$z_1 = z_1 + 1 \tag{1}$$

3. *Relaxation.* If $z_i > z_i^t h$ i relax site i.

For $i = 1$:

$$\begin{aligned} z_1 &\to z_1 - 2, \\ z_2 &\to z_2 + 1 \end{aligned} \tag{2}$$

For $i = 2, ..., L - 1$:

$$\begin{aligned} z_i &\to z_i - 2, \\ z_{i\pm1} &\to z_{i\pm1} + 1 \end{aligned} \tag{3}$$

For $i = L$:

$$\begin{aligned} z_L &\to z_L - 1, \\ z_{L-1} &\to z_{L-1} + 1 \end{aligned} \tag{4}$$

Choose a new threshold slope $z_i^{th} \in \{1, 2\}$ at random for the relaxed site only, i.e. let

$$z_i^{th} = \begin{cases} 1 & \text{with probability } p \\ 2 & \text{with probability } 1 - p \end{cases} \tag{5}$$

using $p = 1/2$. Continue relaxing sites until $z_1 < z_1^{th}$ for all i.

4. *Iteration.* Return to **2**.

The investigation was carried out in a manner of ordered tasked and this is reflected in the structure of this report

2 Implementation of the Oslo Model

A computer program was written to run the above algorithm for systems of easily changing size L. The operation of the routines was validated in the following way: First, a system of size $L = 4$ was initialised and the height, slope and threshold slope at each site where output as arrays of length 4. This system was driven and relaxed once at a time while the mentioned observables were checked by hand. Subsequently, the system was run automatically (driven a number of times N, relaxed recurrently until all $z_i < z_i^{th}$ before each drive) and values where recorded about the height at site 1. The average height was compared to known values (for $L = 16$and 32) successfully which indicated that the model was working properly.

3 Height Investigations

From the definition of the slope as $z_i = h_i - h_{i+1}$ and $h_{L+1} = 0$ we get

$$h(t; L) = \sum_{i=1}^{L} z_i(t). \tag{6}$$

In order to perform the tasks below systems of all the required sizes where initialised and driven while the height $h(t; L)$ was recorded at all times t.

TASK 2a

Starting from an empty system, the total height of the pile was measured as a function of time t for the range of system sizes listed above. The height $h(t; L)$ is plotted vs. time t for the various system is in Figure 1. We see that all systems grow the same until the site $i = L$ topples and the system "realises" that it is finite. Until that point there is nothing to separate the systems and this is very clearly seen in the figure.

TASK 2b

He we are only interested in the scaling behaviour for $L \gg 1$ and hence ignore potential corrections to scaling. We show that for a system of size L in the steady state, the average of the height of the pile over time is expected to scale linearly with system size. For this we need to make the assumption that $\langle z \rangle$ does not vary (or at least does not vary extensively) with system size. Then taking the definition of the average

$$\langle z \rangle = \frac{1}{N} \sum_{i=1}^{N} z_i(t) \tag{7}$$

and replacing N with L we get that $h(t; L) = \langle z \rangle L$. Similarly, we show that the average of the cross-over time $\langle t_c(L) \rangle$ for systems of linear size L to reach the steady state scales with L^2. First, we consider the area of the the pile. When the pile has reached its steady state it will have formed a triangle of height $h(t; L)$ and base L. Hence, the area is given

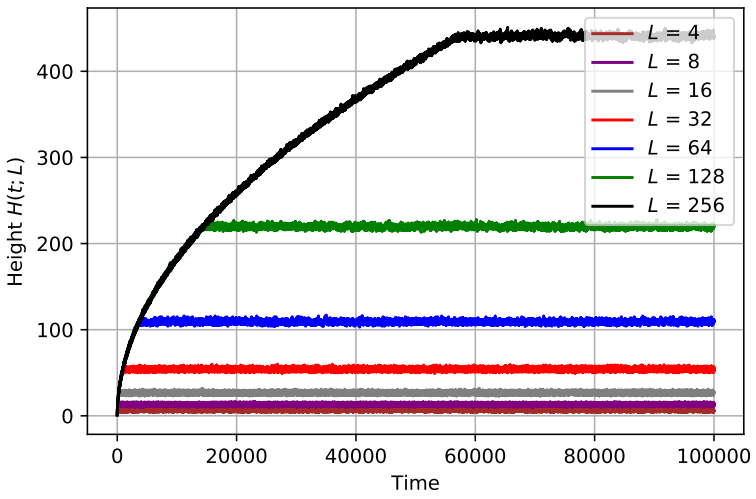

Figure 1: Height $h(t;L)$ for systems of sizes 4,8,16,32,64,128, and 256 is plotted against time. All systems are seen to pass through their transient configurations until they reach the set of recurrent configurations which is the attractor of the dynamics. We see that all systems grow in the same manner until the reach their steady state

by $\frac{height \times base}{2} = \frac{\langle z \rangle L^2}{2}$ by substituting the above expression for height. This means that the pile will contain approximately this many grains. Recalling that time is measured as the amount of grains added to the system and that no grains have left this system until this point the average cross-over time $\langle t_c(L) \rangle$ is proportional to this value.

TASK 2c

For this task systems of each size were realised several times and an average of the height was taken according to:

$$\tilde{h}(t;L) = \frac{1}{M} \sum_{j=1}^{M} h^j(t;L), \tag{8}$$

where $h^j(t;L)$ is the height of the j^{th} realisation of a system of size L at time t. Here, M was set to 10.

Guided by the answers to the two questions in TASK 2b, we produce a data collapse for the processed height $\tilde{h}(t;L)$ vs. time t for the various system sizes. We express this mathematically by introducing

$$\tilde{h}(t;L) = \langle z \rangle L \times \mathcal{F}(2t/\langle z \rangle L^2). \tag{9}$$

At large arguments (x) the scale function $\mathcal{F}(x)$ will equal unity since steady state has been reached and height must equal $\langle z \rangle L$. For small arguments $\mathcal{F}(x)$ must behave in the same way for all systems. Considering a system of a given size as it fills up with grains, we see that the size does play a role until the site $i = L$ topples and hence we expect all

systems to grow in the same way until that point. Guided by Equation 9 we can produce a data collapse by dividing the y-axis by L and the x-axis by L^2. This is shown in figure 2.

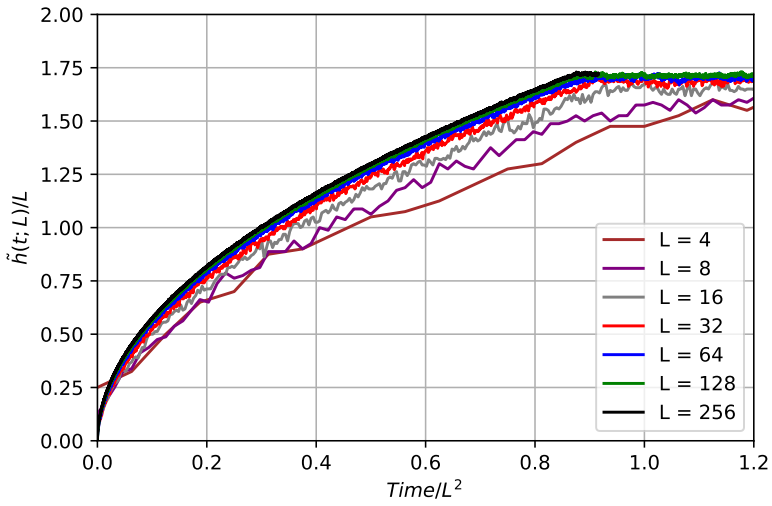

Figure 2: Data Collapse of smoothed height $\tilde{h}(t;L)$ against time. The height axis is divided by L and time by L^2. We see that system sizes 64,128, and 256 are on the same lines while smaller systems diverge because of finite scaling effects. Qualitatively looking at the point where steady state is reached we see that it occurs at approximately $x = 0.85$ which agrees with the prediction that this happens at $\frac{\langle z \rangle}{2}$. An an example we take the measured average slope for system $L = 256$, $\langle z \rangle_{256}/2 = 0.86 \pm 0.01$.

We can now use the form of the data collapse to probe the function $\mathcal{F}(x)$. Theoretically, we have already established that when the pile is at height $h(t;L)$ it will have an area of $\frac{\langle z \rangle L^2}{2}$. Rearranging that to $\frac{h^2}{2\langle z \rangle}$ and recalling that the area corresponds to the time we arrive at $h = (2\langle z \rangle t)^{1/2}$. Informed by this result we can now define the scaling function $\mathcal{F}(x)$ as:

$$\mathcal{F}(x) = \begin{cases} \sqrt{x} & \text{for } x \leq 1 \\ 1 & \text{for } x \geq 1 \end{cases} \tag{10}$$

Having arrived to this we can attempt to fit it to the data and compare the fit coefficients to the prediction. It was decided to do this for the largest system ($L = 256$) to minimise potential corrections to scaling. Since we have divided the y-axis by L and the x-axis by L^2 we expect to see a graph of $h = \sqrt{2\langle z \rangle}\sqrt{(t)}$. This is shown in Figure 3. We can now compare the value of $\langle z \rangle$ slope returned from the fit ($\langle z \rangle_{\text{fit}} = 1.715 \pm 0.003$) to the measured average slope for this system, $\langle z \rangle_{256} = \frac{\langle \tilde{h}(t;256) \rangle}{256} = 1.720 \pm 0.008$, which we obtain by averaging all the measured heights after the system has reached its steady state. We see that the two are in agreement.

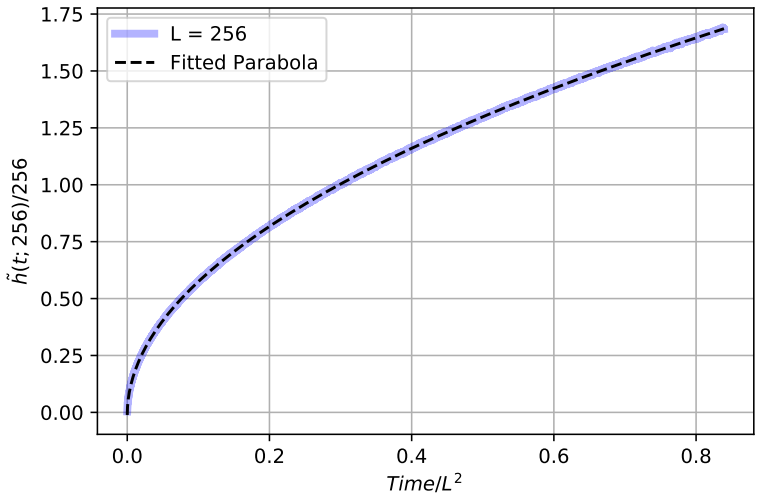

Figure 3: The expression $y = (2\langle z \rangle x)^{1/2}$ is fit to the measured collapsed data for system $L = 256$ with $\langle z \rangle$ as a parameter to be determined. The fit was performed with a χ^2 minimisation routine the the parameter was measured as $\langle z \rangle_{\text{fit}} = 1.715 \pm 0.003$.

TASK 2d

Here, we assume that $\langle z_i \rangle = \langle z \rangle$ in order to show that $\langle t_c(L) \rangle = \frac{\langle z \rangle}{2} L^2(1 + \frac{1}{L})$. The the cross-over time is given by

$$t_c(L) = \sum_{i=1}^{L} z_i \cdot i \tag{11}$$

where the z_i denote the configuration at the moment when the final site is about to topple. Now, the average $t_c(L)$ is given by

$$\langle t_c(L) \rangle = \frac{1}{N} \sum_{j=1}^{N} t_c(L) = \frac{1}{N} \sum_{j=1}^{N} \sum_{i=1}^{L} z_i^j \cdot i. \tag{12}$$

We can rearrange to

$$\langle t_c(L) \rangle = \sum_{i=1}^{N} \sum_{i=j}^{N} \frac{1}{N} z_i^j \cdot i = \sum_{i=1}^{N} \langle z_i \rangle \cdot i \tag{13}$$

Assuming that $\langle z_i \rangle = \langle z \rangle$ this is recast as

$$\langle t_c(L) \rangle = \langle z \rangle \sum_{i=1}^{L} i \tag{14}$$

which is now recognised as the sum of the arithmetic series $a_n = a_1 + (n-1)d$ with $a_n = d = 1$. Using now the standard formula $S_n = \frac{n}{2}[2a_1 + (n-1)d]$ [3] with $n = L$ we arrive at $S_L = \frac{L^2}{2}(1 + \frac{1}{L})$ and hence

$$\langle t_c(L)\rangle = \frac{\langle z\rangle L^2}{2}\left(1+\frac{1}{L}\right) \tag{15}$$

Now, we numerically measure $t_c(L)$ as the number of grains in the system before an added grain induces a grain to leave the system for the first time, starting from an empty system. We do this several times to estimate the average of the cross-over time, $\langle t_c(L)\rangle$. For each system, $t_c(L)$ was measured N_L times. For small systems ($L = 4, 8$), N_L was 1000 but as the system size increased the computation time became longer and longer thus restricting the measurement of $L = 256$ to only 10 times. The cross-over times are plotted against system size in figure 4 a curve of the form of Equation 15 is fitted to them. However, in fitting this curve we have made the assumption that $\langle z\rangle$ is the same

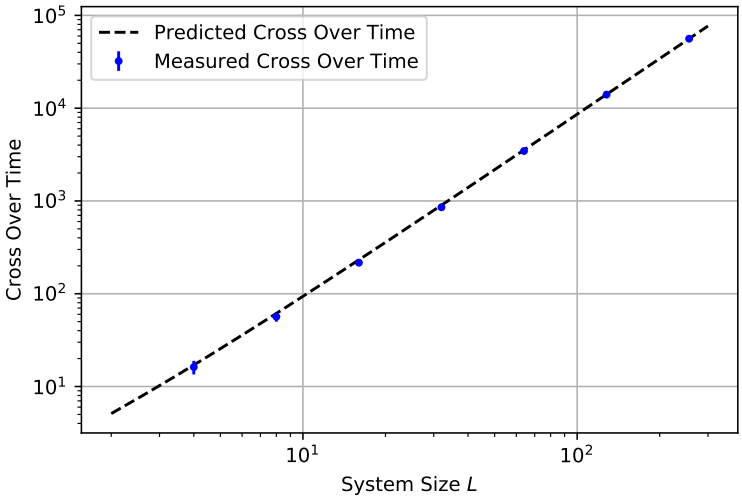

Figure 4: Plot of cross-over time against system size for system of $L = 4, 8, 16, 32, 64$, and 128 and logarithmic scale. The form of Equation 15 is fit to the data by varying $\langle z\rangle$ to minimise χ^2.

for all sizes. This is not justified and was not a condition to the above proof. Hence, a better approach is to measure $\langle z\rangle$ for each system and compare the prediction with the measurement one by one. This approach is shown in Table 1 and indeed verifies the prediction of Equation 15.

TASK 2e

Here we consider the numerical data for the average height $h(t; L)_t$ to investigate whether it contains signs of corrections to scaling. We assume the following form of the corrections to scaling $\langle h(t; L)_t\rangle = a_0 L(1 + a_1 L^{\omega_1} + a_2 L^{\omega_2} + ...)$ where $\omega_i > 0$ and a_i are constants. Neglecting terms with $i > 1$, we attempt to estimate a_0, a_1, and ω_1. The first step is to measure a_0 by rearranging the expression for for $\langle h(t; L)_t\rangle$ to obtain a linear function.

Table 1: Measured and predicted values of cross-over time for various system sizes. Predictions based on measured $\langle z \rangle$ and Equation 15. We see that all values agree within uncertainty and therefore the prediction of equation 15 is verified. The errors quoted refer to the standard error in the case of measured crossover time and an error propagated from the standard error of $\langle z \rangle$ in the predicted case.

System Size	Measured t_c	Predicted t_c
4	16.2 ± 2.7	15.7 ± 2.0
8	56.5 ± 6.5	58.4 ± 4.3
16	216 ± 14	225 ± 10
32	855 ± 38	889 ± 22
64	3454 ± 91	3541 ± 52
128	13990 ± 195	14145 ± 118
256	56043 ± 387	56592 ± 263

The derivation is shown below:

$$\langle h \rangle = a_0 L(1 + a_1 L^{-\omega_1})$$
$$\frac{\langle h \rangle}{L} = a_0 - a_0 a_1 L^{-\omega_1}$$

Now taking the logarithms of both we arrive at

$$log_2(a_0 a_1) - \omega_1 log_2(L) = log_2(a_0 - \frac{\langle h \rangle}{L}) \tag{16}$$

From the above we see that a plot of $log_2(a_0 - \frac{\langle h \rangle}{L})$ against $log_2(L)$ will yield a straight line if the correct value of a_0 is used. We can begin with a first estimate of $a_0 \approx \langle z \rangle_{256} = 1.72$. After some manual tweaking of the parameter we arrive at the range $1.73 - 1.76$. This is illustrated in figure 5-left.

Yet, it is still difficult to isolate the correct value of a_0 accurately. Thus, the r^2 correlation coefficient was used to quantify how straight the line is and a minimization routine was used to find the value of a_0 that minimises the value of $1-r^2$. This is illustrated in Figure 5-right. The final measured value of a_0 is 1.7365. We can now plot Equation 6 again using the measured value of a_0. We can now measure ω_1 from the slopes of this graph and a_1 as $a_1 = \frac{c}{a_0}$ where c is the y-intercept. The results are $\omega_1 = -0.559 \pm 0.008$ and $a_1 = 0.130 \pm 0.026$.

TASK 2f

The scaling of the standard deviation of the height $\sigma_h(L)$ with system size is investigated. The standard deviation of all heights has obtained using the heights measured for the above task. These are plotted in Figure 7-left were it is shown that the standard deviation

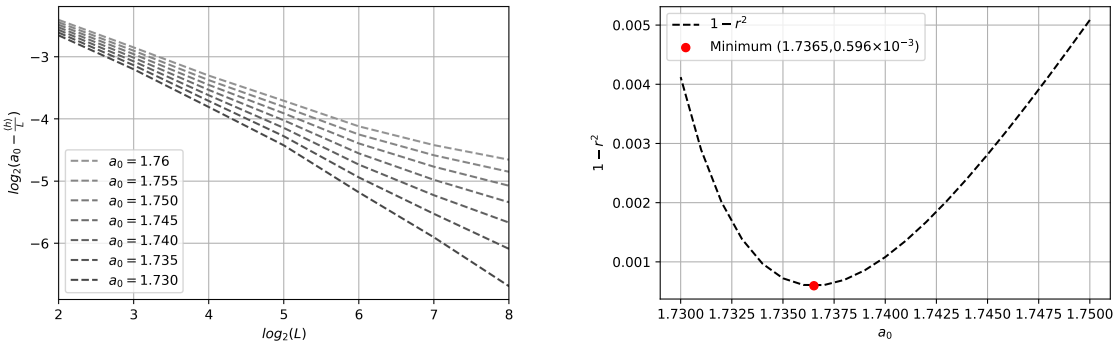

Figure 5: Left: The values $log_2(a_0 - \frac{\langle h \rangle}{L})$ are plotted against $log_2(L)$ for different values of the constant a_0. This serves to illustrate how the variation in a_0 changes the curvature of the plotted. One can imagine that there exists a value of a_0 in that range which produces a straight line. Any logarithm could have been choose, but log_2 was selected to reflect the variation in system site. Right: The value of $1 - r^2$ where r is the correlation coefficient is of the values plotted on the left is plotted against a_0. This curve is minimised using a computational minimization routine to give the value of a_0 which yields the most straight line.

is roughly proportional to $\sigma_h \propto L^\beta$ where $\beta = 0.229 \pm 0.007$.Now we predict what will happen with the average slope and its standard deviation in the limit of $L \to \infty$. Form TASK 2e we see that as $L \to \infty$, $\langle h \rangle$ tends to $a_0 L$ and therefore the average slope will converge on a single value $\langle z \rangle = \langle h \rangle / L = a_0 = 1.7365$. At the same time the standard deviation of the average slope $\sigma_{\langle z \rangle} = \frac{\sigma_h}{L} \propto L^{\beta - 1} = L^{0.771}$ and therefore will tend to zero as $L \to \infty$.

TASK 2g [10 marks]

We consider $h = \sum_{i=1}^{L} z_i$ and ssume that z_i are independent, identically distributed random variables with finite variance. According to the central limit theorem (and as $L \to infty$) we expect the slope to have a Gaussian distribution around the average $\langle z \rangle$. Since $h = z \times L$ we expect $P(h; L)$ to also be a Gaussian probability density function. $P(h; L)$ is plotted for all systems in Figure 8.

Inspired by the theoretical expectation for $P(h; L)$ under the assumptions above, we use the measured values of $\langle h \rangle$ and σ_h to produce a data collapse for the various system sizes of $P(h; L)$. Continuing with the above assumption we can presume that all systems follow

$$P(h; L) = \frac{1}{2\pi\sigma_h} e^{\frac{-(h - \langle h \rangle)^2}{2{\sigma_h}^2}}. \tag{17}$$

This suggests that all system sizes share the common structure

$$P(h; L) = A e^{\frac{-x^2}{2}}. \tag{18}$$

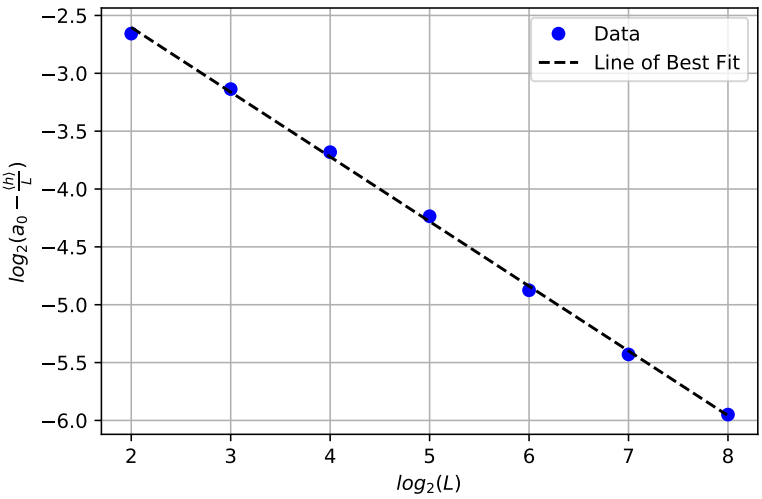

Figure 6: Plot of cross-over time against system size for system of $L = 4, 8, 16, 32, 64,$ and 128. It seen that, although the prediction follows the data, the dashed line is not incorporated within the error bars.

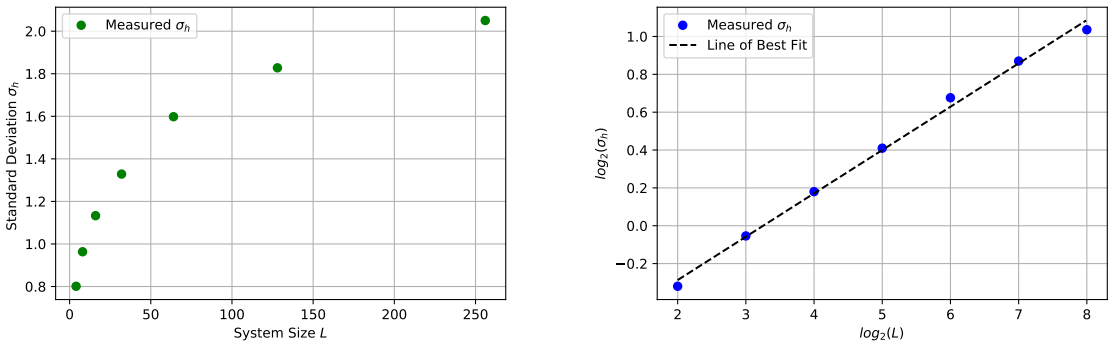

Figure 7: Left: Plot of measured height standard deviation σ_h against system size. We see that σ_h follows an increasing curve with decreasing slope. Right: In order to measure the power relation between σ_h and L the logarithms of the two are plotted and fitted a straight line. This reveals a power relation of the form $\sigma_h \propto L^\beta$ where $\beta = 0.229 \pm 0.007$. Note that we have not proved that this is indeed a power law but have just shown a rough power law-like dependency.

with $A = \frac{1}{2\pi\sigma_h}$ and $x = \frac{h - \langle h \rangle}{\sigma_h}$. Hence, a data collapse was produced by multiplying the $y-$axis with σ_h and plotting it against x[1]. The result is shown in Figure 8.

[1]I.e. subtracting the height by the mean and dividing by the standard deviation

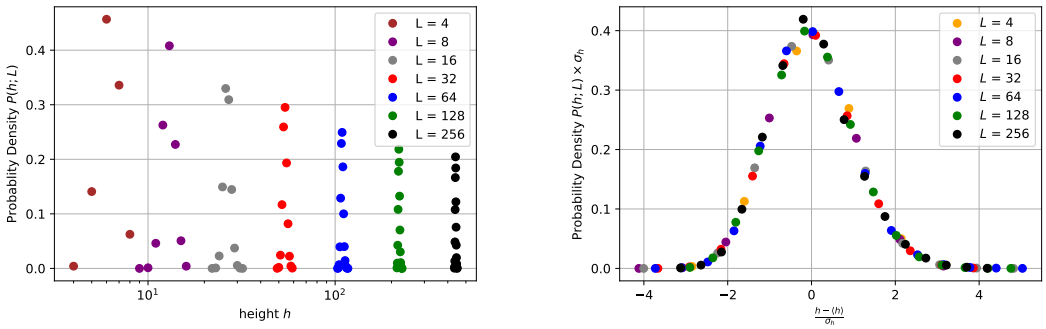

Figure 8: Left: Plot of probability density $P(h;L)$ for systems of $L = 4, 8, 16, 32, 64$, and 128 is semi-log axis. We see that all systems fairly represent Gaussian curves around their average height. Right: Plot of data collapse of probability density $P(h;L)$ for systems of $L = 4, 8, 16, 32, 64$, and 128. We see that all systems collapse to the same curve which resembles a Gaussian distribution.

4 The avalanche-size probability

This part of the project considers measuring the avalanche size probability and its associated moments. The avalanche size s is defined as the number of topplings (relaxations) that are caused by a single addition of a grain at site $L = 1$. The avalanche sizes considered here are only after the system has reached the steady state, i.e we measure only for times $t > t_c(L)$.

The measured normalised avalanche-size probability is defined as:

$$\tilde{P}_N(s;L) = \frac{\text{No. of Avalanches of size s in a system of size L}}{\text{Total no. of avalanches N}} \tag{19}$$

with $\sum_{s=0}^{\infty} \tilde{P}_N(s;L) = 1$.

TASK 3a

Using the log-binned data we plot the avalanche-size probabilities $\tilde{P}_N(s;L)$ vs. avalanche size s for all system sizes with $N = 60000$. Systems of each size where initialised and run until their last site toppled. It is acknowledged that the last site may topple without the system actually having reached real steady state (set of recurrent configurations). Hence after the data is collected the first 1000 avalanches are discarded. Then the data is log-binned and plotted in logarithmic axis in figure 9

TASK 3b

We examine whether the measured $\tilde{P}_N(s;L)$ are consistent with the finite-size scaling ansatz

$$\tilde{P}_N(s;L) \propto s^{\tau_s} G(s/L^D) \text{ for } L \gg 1, s \gg 1, \tag{20}$$

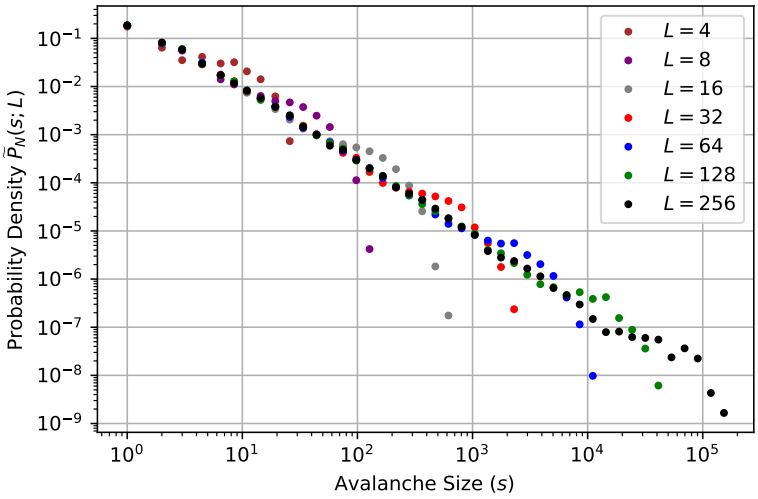

Figure 9: Plot of avalanche-size probability density. The data is seen to behave linearly in the middle range hinting to a pure power law. It is suggested that the deviation from this behaviour is because of finite scaling effects in the $s \to 0$ region and avalanche size saturation towards $s \to \infty$.

and estimate the values of the the avalanche dimension D and the avalanche-size exponent τ_s by performing a data collapse. This is shown in Figure 10. The exponents (D, t_s) where manually adjusted until the data appeared the most uniform. The data was sensitive more to t_s which was estimated to the second decimal place, whereas D could only be estimated to the first. The values are $\tau_s^{collapse} = 1.54 \pm 0.01$ and $D^{collapse} = 2.1 \pm 0.1$.It can be set that the data has collapsed to a satisfactory degree hence verifying the ansatz introduced in Equation 20.

TASK 3c

We measure directly the kth moment $\langle s^k \rangle$ for $k = 1, 2, 3, 4$ where

$$\langle s^k \rangle = \lim_{T \to \infty} \frac{1}{T} \sum_{t=t_0+1}^{t_0+T} s_t^k \tag{21}$$

where s_t is the measured avalanche size at time t and $t_0 > t_c(L)$, that is, the system has reached the steady state. Assuming the finite-size scaling ansatz given in Equation 21 we investigate how the kth moment scale with system size L.We start from an equivalent definition of the k'th moment:

$$\langle s^k \rangle = \sum_{s=1}^{\infty} s^k P(s;L). \tag{22}$$

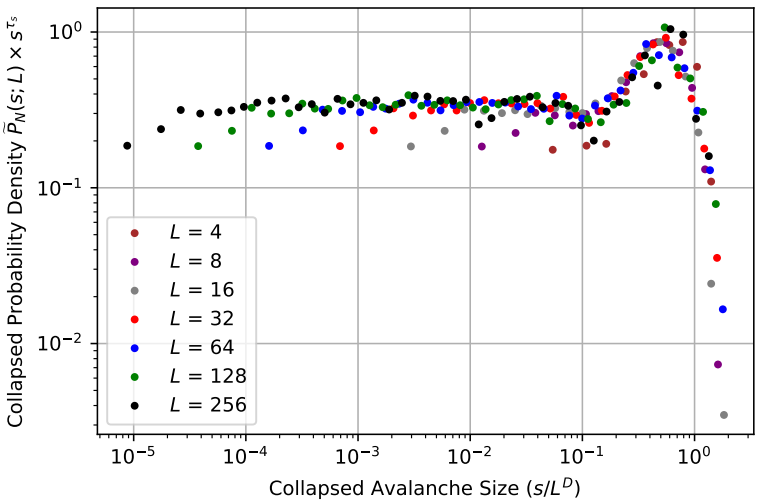

Figure 10: Plot of avalanche-size probability density data collapse. Excluding the initial few points of each system, the data seems to collapse into a single curve, $G(x)$. This is an example of scale free behaviour. The exponents see here are $D = 2.1$ and $\tau_s = 1.54$

From here we substitute the final-size scaling ansatz for the probability distribution and obtain

$$\langle s^k \rangle \propto \sum_{s=1}^{\infty} s^{k-\tau_s} \mathcal{G}(s/L^D.$$

We substitute the summation with an integral by assuming that the main contribution to the moment comes from big sizes ($s \gg 1$),

$$\langle s^k \rangle \propto \int_{s=1}^{\infty} s^{k-\tau_s} \mathcal{G}(s/L^D) ds$$

and finally use the substitution $u = s/L^D$ to obtain

$$\langle s^k \rangle \propto \int_{u=1/L^D}^{\infty} (L^D u)^{k-\tau_s} \mathcal{G}(u) du$$

$$\langle s^k \rangle \propto L^{D(1+k-\tau_s)} \int_{u=0}^{\infty} u^{k-\tau_s} \mathcal{G}(u) du \text{ for } L \gg 1.$$

We observe that the integral is a finite constant for $1 + k - \tau_s > 0$. Hence, the final relationship between the k'th moment and system size is

$$\langle s^k \rangle \propto L^{D(1+k-\tau_s)}. \tag{23}$$

Equation 23 suggests that a plot of the logarithm of $\langle s^k \rangle$ against the logarithm of L will be a straight line through the origin with slope equal to $D(1 + k - \tau_s)$. We plot this in Figure 11-left.

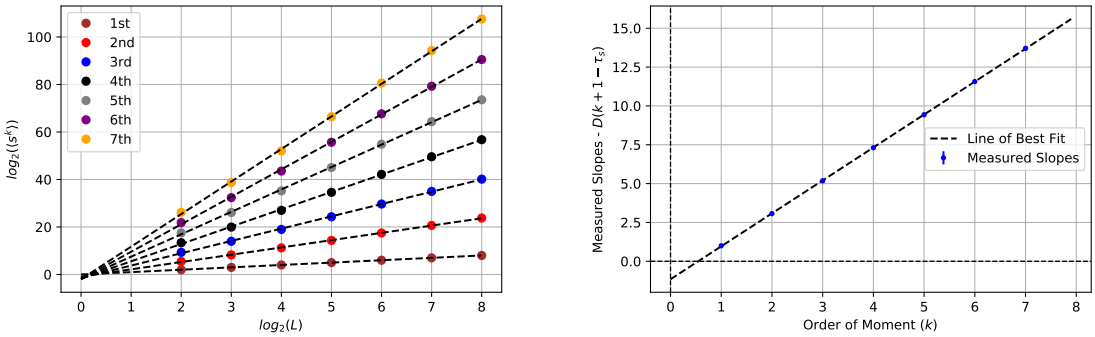

Figure 11: Left: Plot of the logarithm of the k^{th} moment against avalanche size. The plot is a straight line expected by the derived expression (Equation 23). Right: Plot of the measured $D(1+k-\tau_s)$ against k. The plot is a straight line which is used to obtain values for D and τ_s.

The data seem to resemble a straight line well but their measured y-intercepts are not zero. This is clearly indicated in the figure with the smallest intercept being that for $k = 1$, $(-0.462 \pm 1.98) \times 10^{-3}$ and largest for $k = 6$, -2.01 ± 0.53. While the former is zero with the error the later is certainly not[2]. Thus, it can be said that the data is consistent with the prediction of the scaling due to its linearity but not completely because of the finite y-intercept.

Nonetheless, which we can still leverage the above to measure D and τ_s. The slopes from figure 11-left where used to obtain values for D and τ_s by plotting the them against k. Looking at $slope = D(1+k-\tau_s)$ we see that this plot will be a straight line with slope equal to D and $y - intercept$ equal to $1 - \tau_s$. This is plotted in Figure 11-right resulting to $D^{moment} = 2.120 \pm 0.005$ and $t_s^{moment} = 1.55 \pm 0.01$. We can compare this to the previous measurements ($D^{collapse} = 2.1 \pm 0.1, \tau_s^{collapse} = 1.54 \pm 0.01$) to see that the two are in agreement. Yet, our prediction is not fully accurate because of the finite $y-$intercepts in Figure 11-left, a likely cause of which are corrections to scaling.

5 Conclusion

A computational implementation of the Oslo Model was successfully run for system sizes from $L = 4$ to 256. The systems successfully demonstrated the key property of the Oslo Model, i.e. self-organised criticality. They were driven by a very simple and regular stimulus (addition of one gray) and yet reached a steady state were avalanches of all possible sizes were observed. The concept of data collapse was applied both at measuring height and avalanche size. The latter facilitated to show that the Oslo Model displays scale-fee behaviour which is an important propery of critical systems.

[2]The errors here as obtained from the χ^2 minimisation routine used to fit the straight line.

References

[1] K. Christensen, A. Corral, V. Frette, J. Feder, and T. Jossang, "Tracer dispersion in a self-organized critical system," *Physical Review Letters*, vol. 77, no. 1, pp. 107–110, 1996.

[2] K. Christensen, *Complexity Project Notes*. Imperial College - Centre for Complexity Science, 2019.

[3] *Blackett Laboratory Mathematical Formulae*. Imperial College - Blackett Laboratory, https://www.imperial.ac.uk/media/imperial-college/faculty-of-natural-sciences/department-of-physics/internal/students/current/ug/exams.